Error assessment in post-necking strain hardening behaviour identification of mild steel sheet

S. Coppieters[a], T. Hakoyama[b], K. Denys[a], D. Debruyne[a] and T. Kuwabara[b]

[a] Department of Materials Engineering, KU Leuven, Technology Campus Ghent, Gebroeders De Smetstraat 1, 9000 Ghent, Belgium.
[b] Division of Advanced Mechanical Systems Engineering, Institute of Engineering, Tokyo University of Agriculture and Technology, 2-24-16, Nakacho, Koganei-shi, Tokyo 184-8588, Japan.

sam.coppieters@kuleuven.be

Abstract. The information hidden in the diffuse neck of a tensile test on a thin metal sheet can be extracted using a special case of the non-linear virtual fields method yielding the so-called post-necking strain hardening behaviour. The method, however, requires a number of assumptions which are scrutinized in this paper. To eliminate experimental errors which could potentially hamper the assessment, virtual test data (i.e. strain fields at different load steps) is generated using a FE model of the tensile test. The identification strategy is then used to retrieve the reference strain hardening behaviour used in the FE simulation. This approach is used to study the necessity of incorporating rate-dependent plasticity in the identification procedure. Additionally, the necessary plane stress condition in the diffuse neck is studied.

1. Introduction

Pioneering work of Bridgman [1] resulted in a solution for the problem of diffuse necking. Bridgman considered his method a second level of approximation because the method is only concerned with the distribution of stress and strain across the diffuse neck. He also envisioned a third level of approximation, also referred to as the "complete solution" of the general problem, which takes the material state and the shape of the whole deforming specimen into account. Several researchers arrived at such complete solutions using finite-element based inverse methods. In order to avoid the shortcomings of the FE-based inverse method, a method based on the complete solution to retrieve the strain hardening behavior hidden in the diffuse necking regime was presented in [2,3]. The key point in this method is that the strain hardening behavior can be identified by minimizing the discrepancy between the internal and the external work in the region where the diffuse neck develops. The method is a special case of the Virtual Fields Method (VFM) [4]. The initial assumption [2] that an increase of the cost function caused by an error in the work hardening law is significantly larger than an increase caused by an error in the (anisotropic) yield criterion was investigated in [5]. In this contribution, two additional assumptions are scrutinized: a) the necessary plane stress condition in the diffuse neck and b) rate-independent plasticity.

2. Methodology

The Post-Necking Tensile Experiment (PNTE) is simulated using Abaqus/Standard. The computed surface strains, elongation of the monitored diffuse necking zone and the tensile force are used as input for the identification method presented in [2,3]. This approach excludes all experimental errors and enables studying the impact of the assumptions on the identified parameters. The simulation of the PNTE was performed using an appropriate material model for a mild steel sheet [6] with an initial thickness of 0.65 mm. The tensile test is simulated with a constant cross-head speed of 0.05 mm/s. The geometry of the specimen has a width of 20 mm and complies with [7]. The surface strains are extracted from a central zone (length 50 mm) around the diffuse neck. Virtual data is generated at a measurement frequency of 2Hz. The inverse identification [2,3] uses rate-independent plasticity with the von Mises yield criterion and the p-model [3] to describe isotropic hardening:

$$\sigma_{eq} = \begin{cases} K(\varepsilon_0 + \varepsilon_{eq}^{pl})^n & \textbf{if } \varepsilon_{eq}^{pl} \le \varepsilon_{\max} \\ K(\varepsilon_0 + \varepsilon_{\max})^n + Q[1 - e^{-p(\varepsilon_{eq}^{pl} - \varepsilon_{\max})}] & \textbf{if } \varepsilon_{eq}^{pl} > \varepsilon_{\max} \end{cases} \quad (1)$$

where ε_{max} is the maximum uniform strain and p the post-necking hardening parameter.

2.1. Strain rate dependency

When uniform straining ceases the strain rate gradually increases within the diffuse neck. In [3] the strain rate in the central point of diffuse neck was measured using DIC and the maximum strain rate was about 0.02 $\frac{1}{s}$. It was, however, assumed in [3] that since very few material points violate the quasi-static upper limit of 0.01 $\frac{1}{s}$, the impact on the globally identified strain hardening behavior could be ignored. The virtual data was simulated using a plane stress (shell elements) FE model incorporating rate-dependent plasticity. The von Mises yield criterion along with a rate-dependent hardening model was used:

$$\sigma_{eq} = g(\varepsilon_{eq}^{pl}) \left(\frac{\dot{\varepsilon}_{eq}^{pl}}{0.0005} \right)^m \quad , \; g(\varepsilon_{eq}^{pl}) = 541(0.0036 + \varepsilon_{eq}^{pl})^{0.25} \quad (2)$$

with the exponent m equal to 0.01. Subsequently, rate-independent plasticity was used in the identification procedure to retrieve the strain hardening behavior described by the p-model. A minimum (during uniform elongation) and maximum (in the diffuse neck) plastic strain rate of $\dot{\varepsilon}_{eq}^{pl} = 0.0003\ s^{-1}$ and $\dot{\varepsilon}_{eq}^{pl} = 0.01\ s^{-1}$ was numerically predicted, respectively. Figure 1 shows the reference flow curves Eq.(2) according to those two extreme values of the plastic strain rate $\dot{\varepsilon}_{eq}^{pl}$. The p-model uses the maximum uniform strain $\varepsilon_{max} = 0.23$ obtained from the tensile test. The post-necking hardening parameter p enables to describe a Swift type (small p-value) or a saturation type (large p-value) post-necking strain hardening. It can be inferred from figure 1 that up to $2\varepsilon_{max} \approx 0.47$ the identified p-model is in close agreement with the reference hardening with $\dot{\varepsilon}_{eq}^{pl} = 0.0003\ s^{-1}$. The latter suggests that the influence of the strain rate up to $2\varepsilon_{max}$ can be safely ignored. Indeed, it can be observed from figure 2 that the change of strain rate between $\varepsilon_{eq}^{pl} = \varepsilon_{max}$ and $\varepsilon_{eq}^{pl} = 2\varepsilon_{max}$ is small. Figure 2 shows the evolution of the strain rate for different material points as a function of the elongation of the central region around the diffuse neck. Three different locations are shown: inside the diffuse neck, just outside the diffuse neck (I) and far away from the diffuse neck (II). After the onset of diffuse necking, the strain rate drops at material points far away from the diffuse neck (II). Close to the diffuse neck (II) the strain rate increases, but by approaching $\varepsilon_{eq}^{pl} = 2\varepsilon_{max}$, the strain rate eventually drops. The drop in strain rate is accompanied with further (limited) plastic deformation.

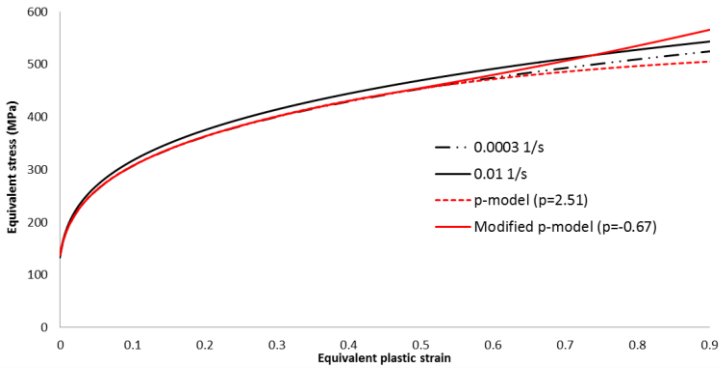

Figure 1. Reference flow curve Eq.(2) for different strain rates. Identified strain hardening models.

The latter means that during this drop the local flow stress is affected by the local instantaneous strain rate level. Clearly, the p-model is not flexible enough to capture the interplay of strain rates within the specimen affecting the local flow stress. Figure 2 also shows the difference between the virtual external work W_{ext} and the computed internal work W_{int} obtained with the identified strain hardening behaviour. It can be concluded that strain rate sensitivity hampers the identification of the rate-independent p-model. However, given that the strain rate change is moderately low between ε_{max} and $2\varepsilon_{max}$, the p-model can be modified in such a way that it responds to the strain rate effect. To do so, ε_{max} in Eq.(1) is changed to $2\varepsilon_{max}$ which is in accordance with observation that the development of transverse stresses is postponed to $\varepsilon_{eq}^{pl} = 2\varepsilon_{max}$ [8]. Figure 1 shows that the modified p-model has a negative p-value signifying a strong increase in strain hardening rate. The predicted W_{int} using the modified p-model is in close agreement with W_{ext}, see figure 2.

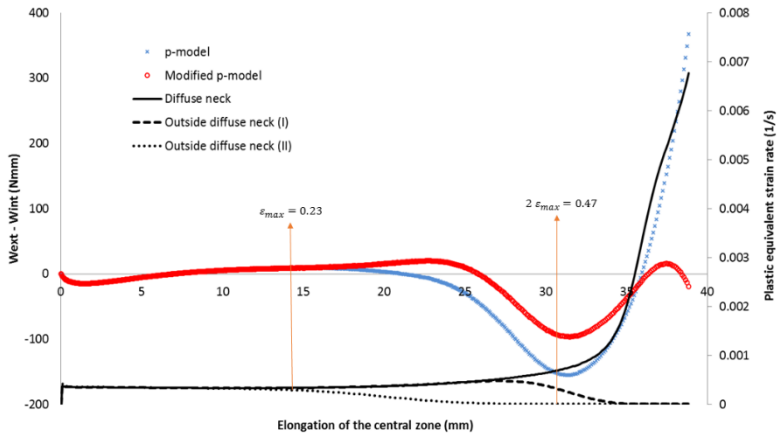

Figure 2. Discrepancy between virtual external work and computed internal work using the identified hardening models. Evolution of strain rate within the tensile specimen at 3 different locations.

2.2. Plane stress conditions

In practice, the surface strains are measured Digital Image Correlation. The volume of the specimen is assumed to remain constant so that the thickness strain can be computed using the measured surface strains. As such, out-of-plane shear strains are neglected and a plane stress state is assumed. The effect of these assumptions is studied by generating virtual data using a 3D (solid elements) FE model, thereby ignoring strain-rate sensitivity. Subsequently, the identification procedure [2,3] is used to retrieve the reference strain hardening model used in the simulation. The black solid curve in Figure 3 shows the

reference strain hardening curve (labelled as *Ref Swift*). It can be inferred that the p-model identified based on the virtual data generated by the 3D FE model (labelled as *P-model (solids)*) deviates from the reference curve at large plastic strains. The latter suggests that the stress state in the diffuse neck differs from plane stress. To check this, the p-model (labelled as *P-model (plane stress)*) was also identified based on virtual data generated by a plane stress FE model. An identical deviation in the post-necking regime, however, was found. Consequently, the origin of this discrepancy cannot be attributed to a deviation from plane stress within the diffuse neck.

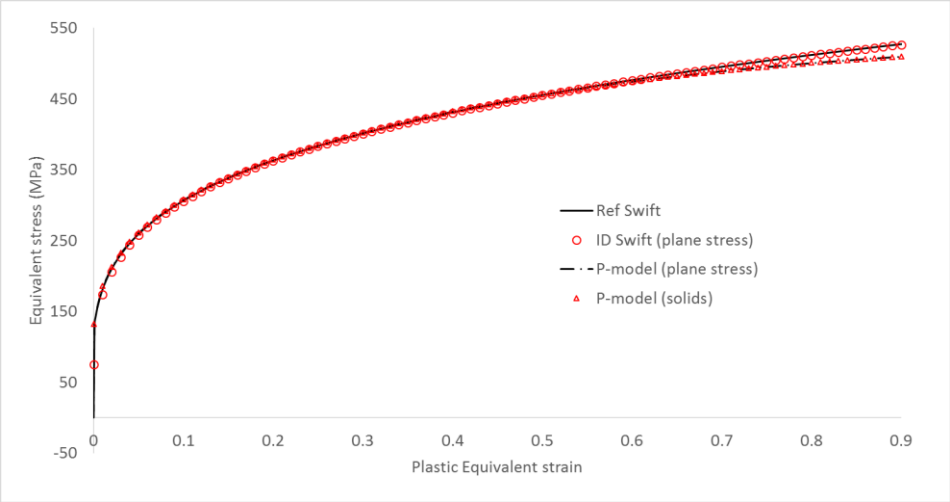

Figure 3. Influence of the stress state in the diffuse neck on the identified strain hardening behaviour.

3. Conclusions

This paper shows that strain rate effects cannot be ignored when identifying post-necking strain hardening behaviour of mild steel sheet. Plane stress conditions, however, within the diffuse neck can be safely assumed.

References

[1] P.W. Bridgman, Studies in Large Plastic Flow and Fracture, McGraw-Hill, NY, 1952.
[2] S. Coppieters, S. Cooreman, H. Sol, P. Van Houtte, D. Debruyne, Identification of the post-necking hardening behavior of sheet metal by comparison of the internal and external work in the necking zone, Journal of Materials Processing Technology, 211 (3), pp. 545-552, 2011.
[3] Coppieters, S., Kuwabara, T. (2014). Identification of Post-Necking Hardening Phenomena in D3uctile Sheet Metal. *Experimental Mechanics* (54), 1355-1371.
[4] J.-H. Kim, A. Serpantié, F. Barlat, F. Pierron, M.-G. Lee, Characterization of the post-necking hardening behaviour using the virtual fields method, International Journal of Solids and Structures, 50, pp. 3829-3842, 2013.
[5] Coppieters, S., Ichikawa, K., Debruyne, D., Kuwabara, T. (2014). Identification of Post-Necking Hardening Behaviour of Sheet Metal: Influence of the Yield Function. International Conference on Experimental Mechanics. Cambridge (UK), 7-11 july 2014.
[6] Ichikawa K., Kuwabara T., Coppieters S., Forming Simulation Considering the Differential Work Hardening Behavior of a Cold Rolled Interstitial-Free Steel Sheet, Key Engineering Materials, 611-612, pp.56-61(2014).
[7] ASTM Standard E8M-96, 1996. Standard test methods for tension testing of metallic materials [metric]. Annual Book of ASTM Standards, Vol. 03.01:76-96.
[8] Iadicola, M.A., 2011. Validation of uniaxial data beyond uniform elongation. AIP Conference Proceedings, 1383, 742-749.